Diffraction at the LHC

A. Kaidalov
ITEP, Moscow

HERA-LHC
Workshop
21 March 2005

Contents:

• Introduction.

- Two complementary views on diffraction
- S-channel view of diffraction.

Absorption of an initial wave due to many inelastic channels leads by unitarity to diffractive elastic scattering.

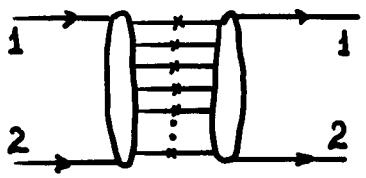

Diffraction is a process, which has a long lifetime $\tau \sim E_L/\mu^2$

E. Feinberg. I. Ya. Pomeranchuk

Diffractive production

Example Dissociation of a deutron

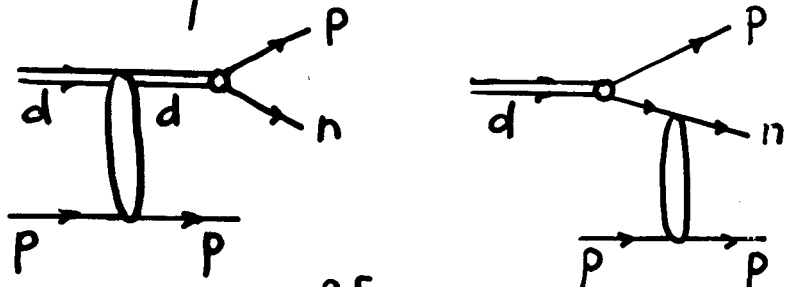

$$\Delta t \approx \frac{2E_L}{M^2 - m_d^2}$$

Inelastic diffraction is due to a difference of amplitudes and is smaller compared to elastic scattering.

Dissociation of a hadron into $q\bar{q}$-pairs (color dipoles).

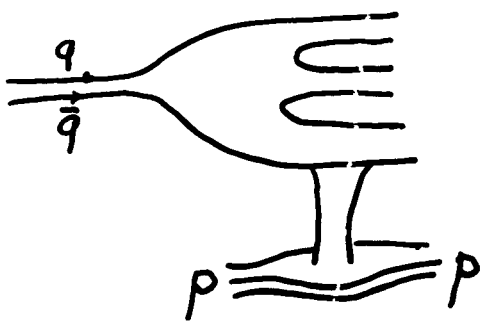

Good and Walker interpretation of diffraction.

M.L. Good, W.D. Walker (1960)

Diffractive part of S-matrix $iD_{ik}(s,b)$ (b: impact parameter) can be diagonalized by an orthogonal matrix Q

$$D = Q F Q^T \quad ; \quad F_{ij} = F_i \delta_{ij}$$

$$\Psi_i = \sum_k Q_{ik} \varphi_k \quad ;$$

Ψ_i - initial state.

φ_k - eigenstates, which have only elastic scat. ↕ Quark configurations with fixed transverse separations.

After diffractive scattering (with $\hat{F} \neq \hat{I} \cdot F$) a final state is a new superposition of eigenstates and thus contains Ψ_i (with $i = 1, 2, \ldots, N$)

Analog of $K_L \to K_S$ regeneration, where K^0 and $\bar{K}^0$ are 'diagonal' states.

If all $F_i = \frac{1}{2}$ ($b \leq R$) - black disc limit - inelastic diffraction is absent.

For $F_i \leq \frac{1}{2}$

$$\sigma^{(el)}(b,s) + \sigma_D^{(in)}(b,s) \leq \frac{1}{2} \sigma^{(tot)}(b,s)$$

Pumplin's bound

$$\left(\sigma^{(i)}(s) = 4\int \sigma^{(i)}(b,s)\,d^2b\right)$$

At $\sqrt{s} \approx 1$ TeV and for $b \approx 0$ $\sigma^{(el)} \approx \frac{1}{2}\sigma^{(tot)} \approx \frac{1}{4}$

$$\sigma_D^{(in)} \lesssim 0.01$$

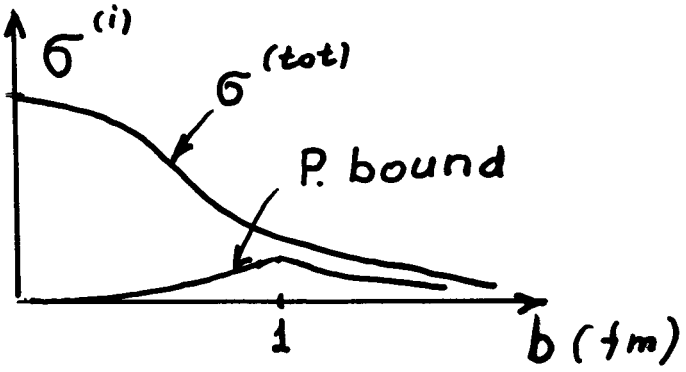

Diffractive production is peripheral in b.

Strong influence of unitarity effects.

Dependence on s, b ?

t-channel view of diffraction

In the Regge pole model diffractive processes can be described by the leading factorizable Regge pole with the vacuum quantum numbers - Pomeron.

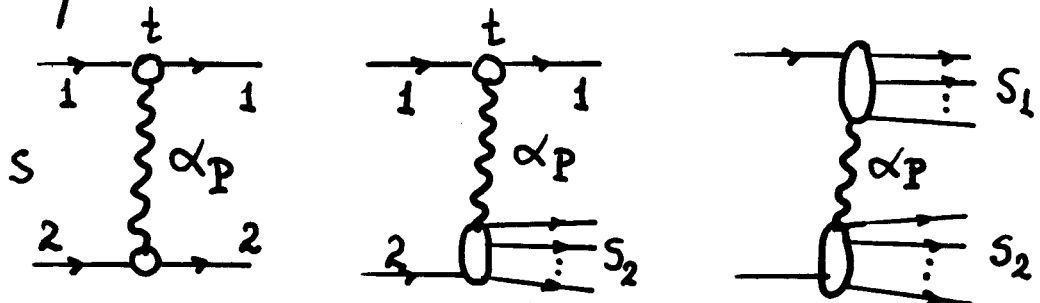

elastic

single dif. dissoc.

double dif. dissoc.

P plays a role of exchanged "particle". Pomeron "flux" is introduced sometimes.

In b-space Regge amplitudes have a gaussian form.

Note that the Pomeron is very non-local object. It corresponds to the process with $\tau \sim E/m^2$.

Pomeron with intercept $\alpha_P(0) > 1$ leads to a violation of unitarity ($s \to \infty$).

Regge cuts (multi-pomeron exchanges in the t-channel) restore s-channel unitarity.

Gribov's technique for evaluation of cuts contributions

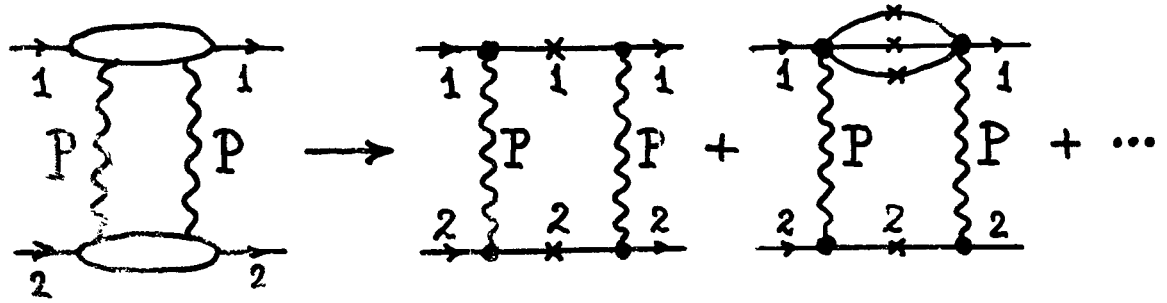

Becomes equivalent to GW formulation, but with known s-dependence

Multipomeron contributions to elastic amplitudes are related to amplitudes of diffractive processes.

For inelastic diffraction effects of multipomeron cuts are even more important.

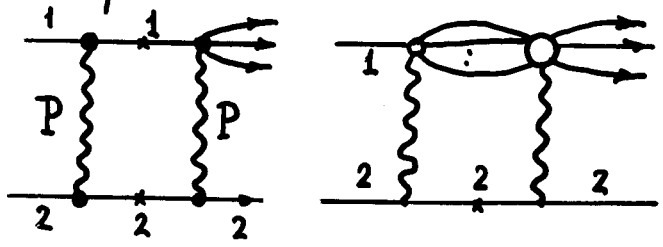

They lead to a peripheral form of amplitudes in b-space.

Gribov diagramme technique and AGK-cutting rules allow for systematic study of multipomeron cuts in diffractive processes and multiparticle production.

Thus an investigation of diffractive processes gives an information on structure hadronic fluctuations and a mechanism of high energy interactions.

- Different high-energy regimes.

a) "Weak coupling" regime.

$$\sigma^{(tot)} \to \text{Const} \quad s \to \infty$$

Following conditions should be satisfied:

i) All inelastic vertices for P vanish as $t \to 0$ $\quad g^{P}_{aX}(t, M_X) \to 0 \quad t \to 0$

Not observed at present. Should be tested at LHC

ii) All elastic coupling of P are the same.

b) "Critical" pomeron.

After renormalization due to selfinteractions

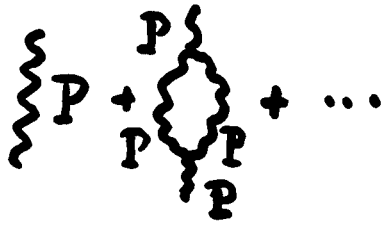

$$\alpha_P(0) = 1$$

$$\sigma^{(tot)} \underset{s \to \infty}{\sim} (\ln s)^{\gamma}, \quad \gamma < 2 \quad \left(\gamma \sim \tfrac{1}{6}\right)$$

Migdal, Polyakov, Ter-Martirosyan

There are no theoretical reasons (at present) for conditions of regimes a) and b) and behavior of $\sigma^{(tot)}(s)$ is not supported by experiment.

Most probable regime:

c) "Supercritical" pomeron (SP)

$$\alpha_P(0) > 1 \quad (\Delta \equiv \alpha_P(0) - 1 > 0)$$

$$\sigma^{(tot)} \sim \ln^2 s \,, \quad s \to \infty$$

Models based on SP give a good description of $\sigma^{(tot)}(s)$, $\frac{d\sigma^{(el)}}{dt}(s,t)$ and other characteristics of high-energy interactions.

Note that the slope of diffraction cone $B \sim \ln^2 s$ in this theory.

This should be seen at LHC

Figure

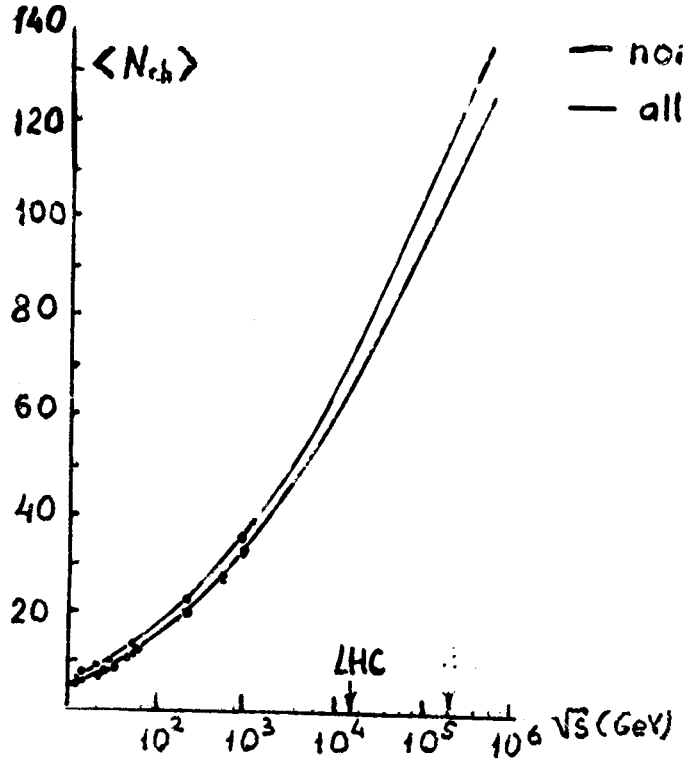
140
120
100
80
60
40
20
⟨N_ch⟩
— non diff.
— all inel.
LHC
10²
10³
10⁴
10⁵
10⁶
√s (GeV)

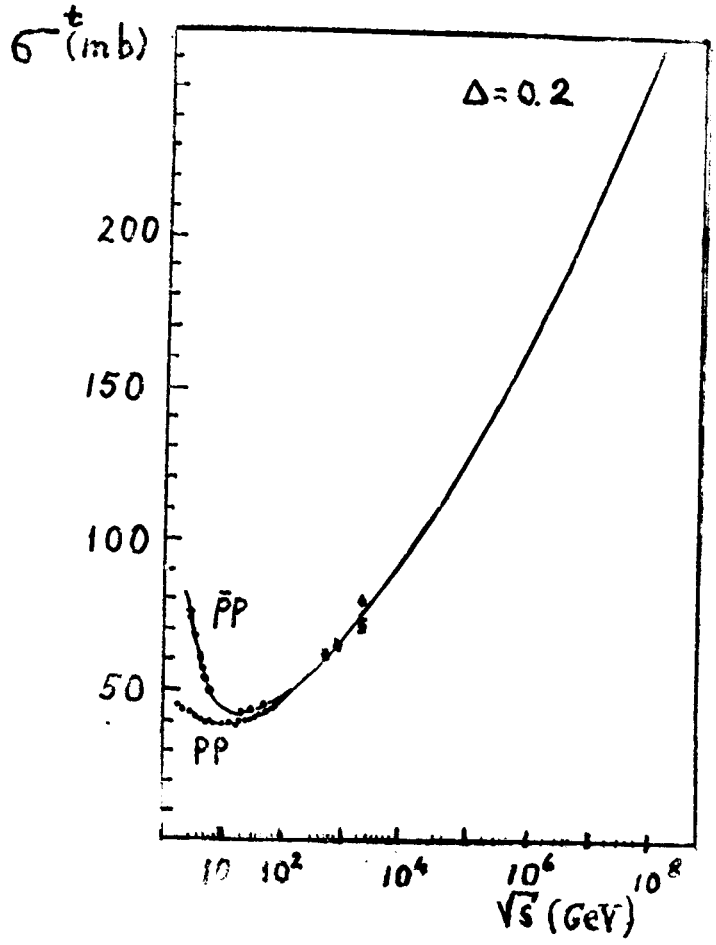
σ_t (mb)
Δ=0.2
200
150
100
50
p̄p
pp
10
10²
10⁴
10⁶
10⁸
√s (GeV)

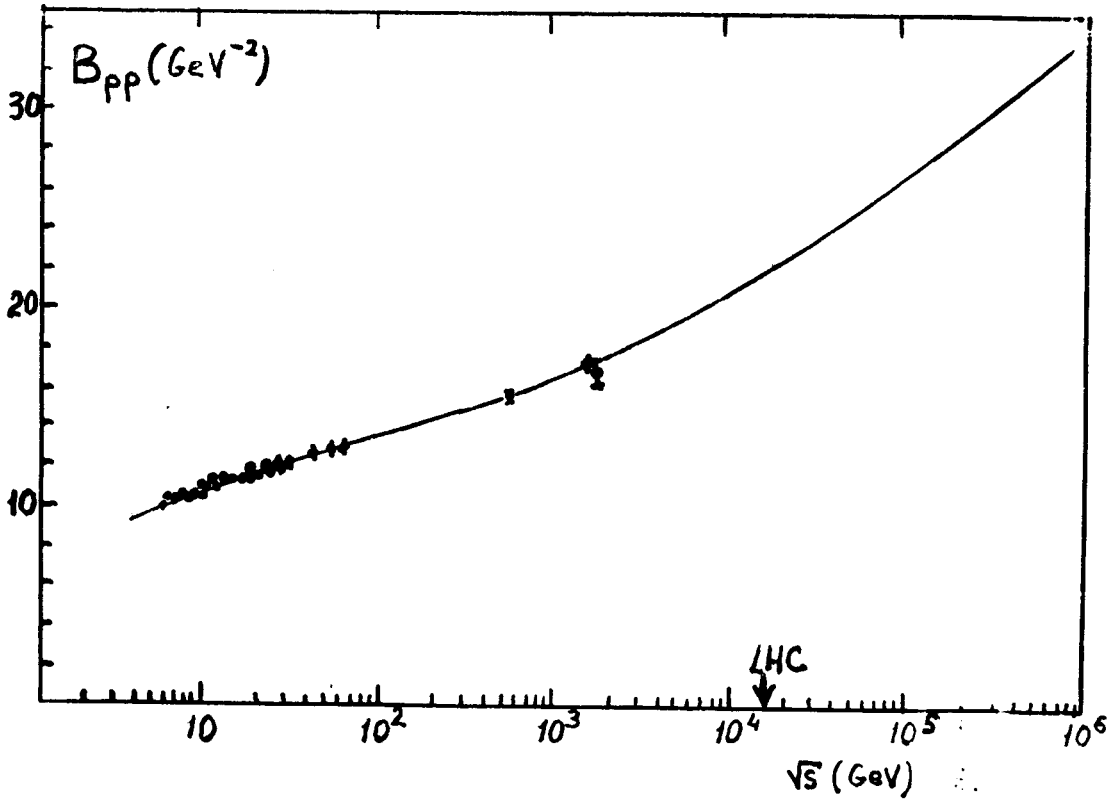
B_pp (GeV⁻²)
30
20
10
LHC
10
10²
10³
10⁴
10⁵
10⁶
√s (GeV)

Fig.1

- Unitarity effects for diffraction.

a) Rise with energy of σ^{SD}, σ^{DD}

In the regge-pole approximation diffractive production of hadronic state with large mass is described by triple-pomeron diagram

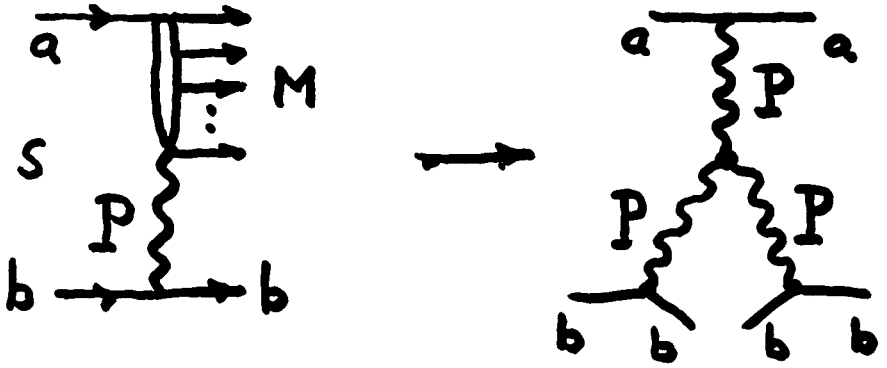

For SP it increases as $s^{2\Delta}$, i.e. faster than $\sigma^{(tot)} \sim s^{\Delta}$.

Same for diffractive production of two large masses

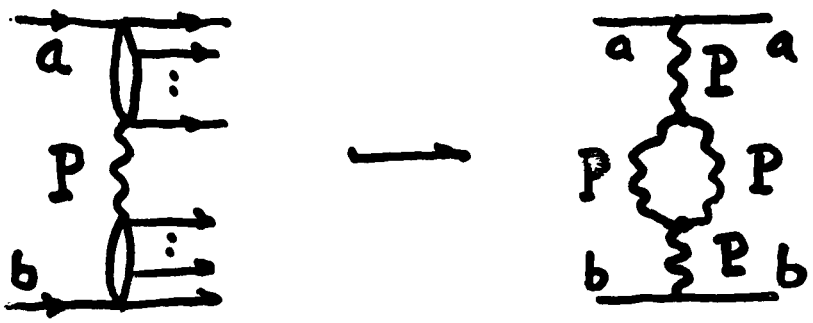

Diffractive production in hadronic interactions.

In the simplest triple-Regge model too fast increase with energy of σ^{SD} is predicted. Account of rescattering allows one to obtain a reasonable description of experiment even with $\Delta \approx 0.2$ ($\Delta \equiv \alpha_{I\!P}(0) - 1$)

(A.K., L.Ponomarev, K.A.Ter-Martirosyan) 1986

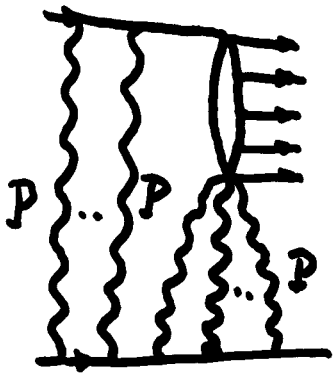

$$\frac{\sigma^{SD}}{\sigma^{(tot)}} \to 0 \sim \frac{1}{\ln \frac{s}{s_0}} \qquad s \to \infty$$

This is due to a peripher. property of inelastic diffract. at very high energies

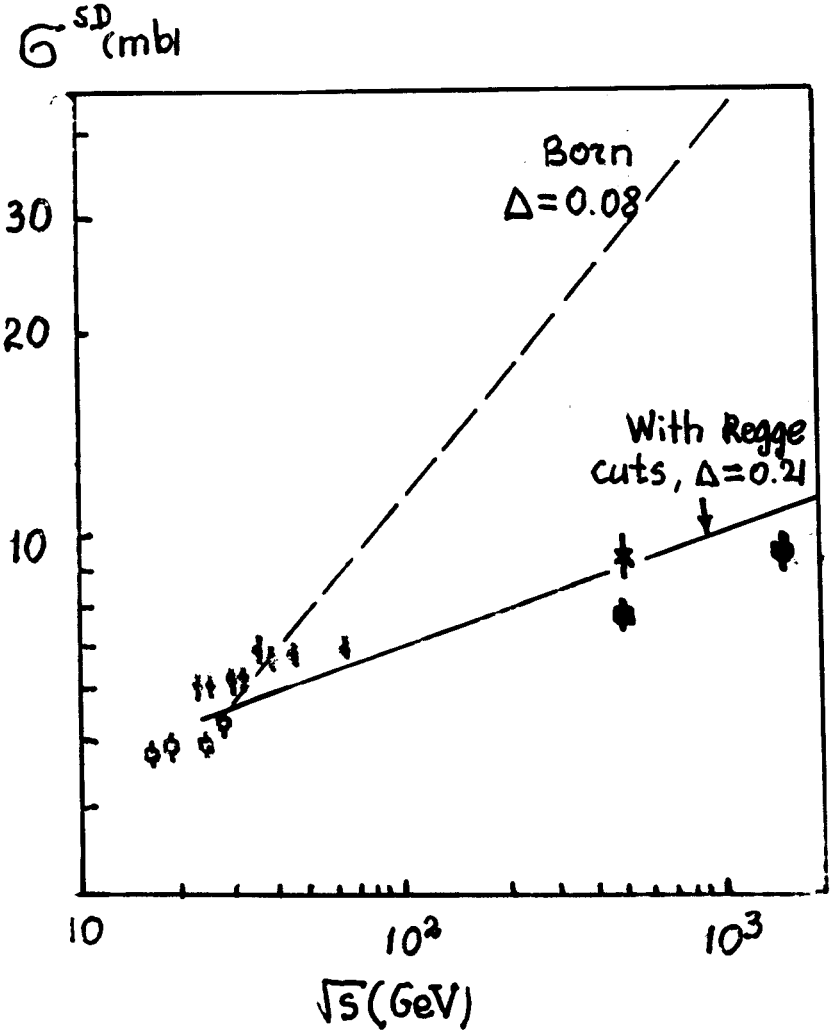

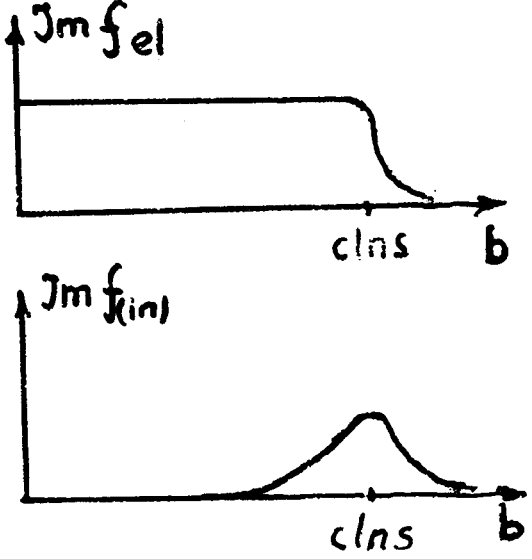

Multigap configurations

Double gap(DPE)

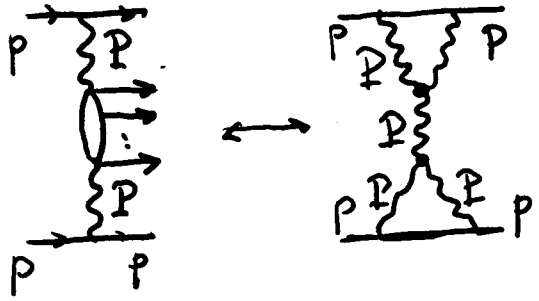

$\sigma_{DPE} \sim 0.4$ mb at LHC

(With account of absorption)

Multigap

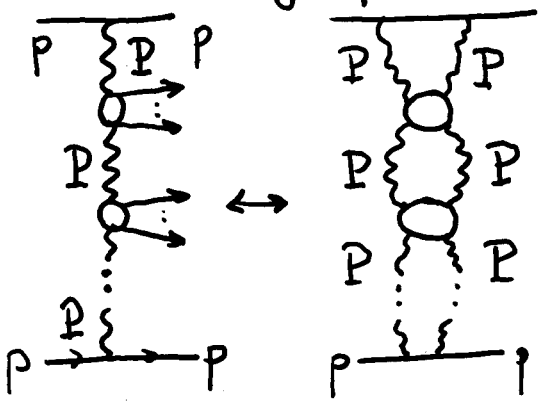

at LHC

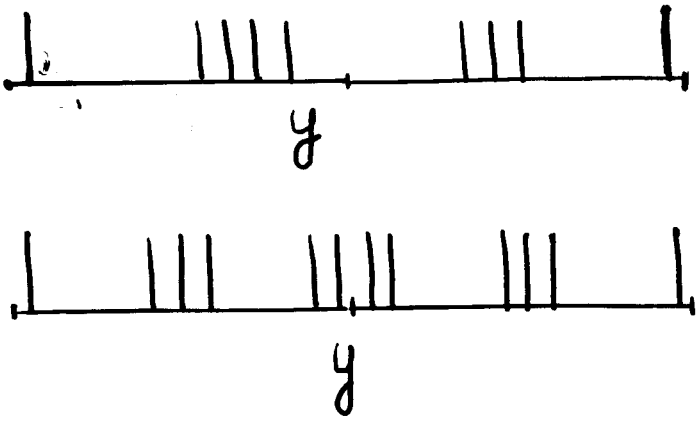

Up to 4 gaps with $\Delta y_i \geqslant 3$

Cross sections of these processes provide important constraints on theoretical models.

• Hard diffraction in hadronic collisions.

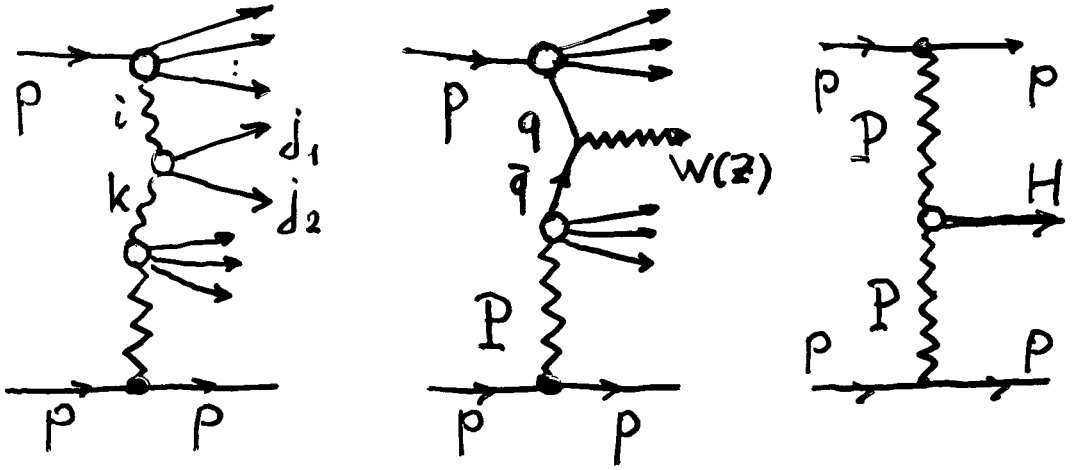

Ingelman, Schlein approximation

Distributions of partons from the pomeron are determined from diffractive DIS

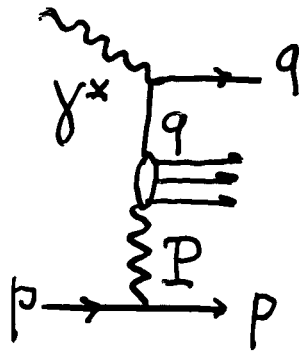

Large uncertainties in $f_{P}^{g}(\beta, Q^2)$ (especially at $\beta \sim 1$)

Discrepancies ~10 with Tevatron data

However rescatterings are important. They reduce cross sections.

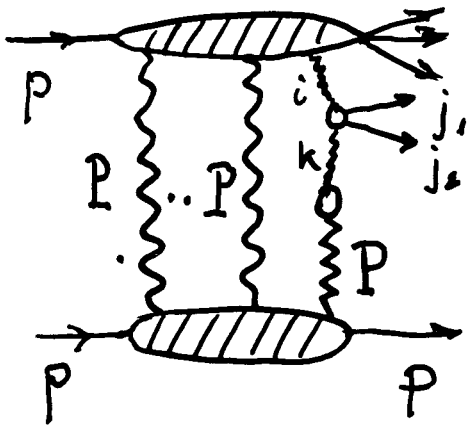

QCD fits of $F_2^{D(3)}$ data

Extraction of the gluon and quark densities in the pomeron from a DGLAP fit to H1 data

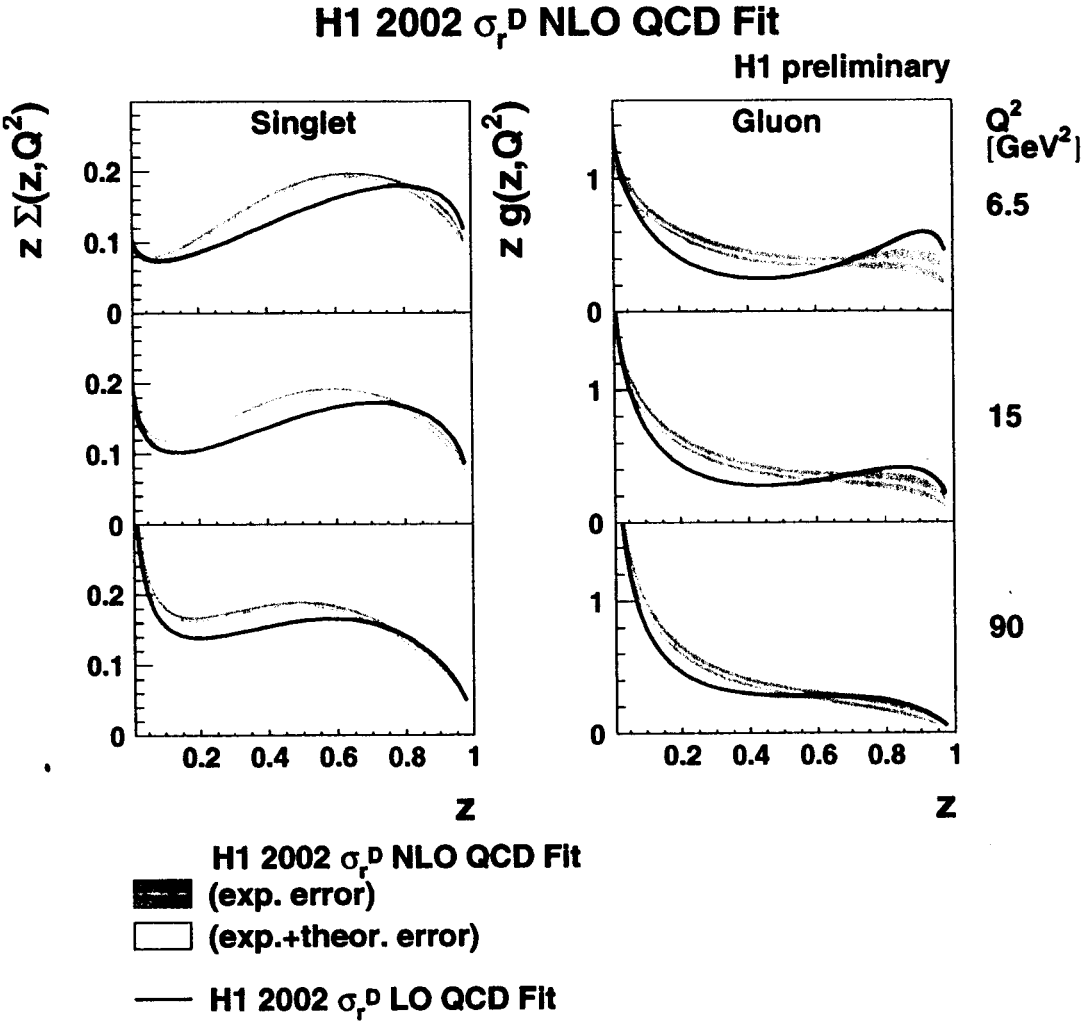

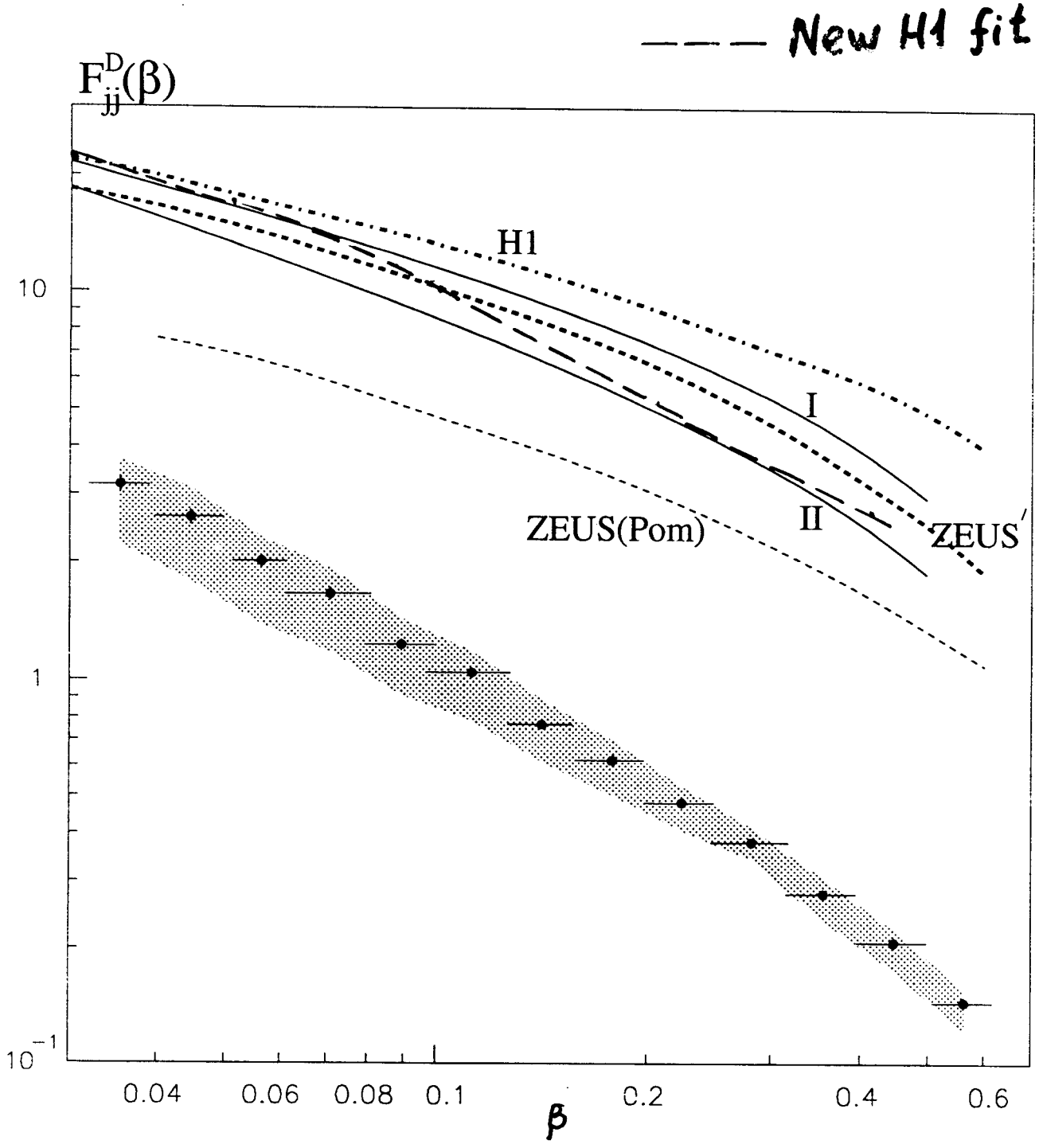
New H1 fit
$F_{jj}^{D}(\beta)$
H1
I
II
ZEUS(Pom)
ZEUS'
10
1
10^{-1}
0.04
0.06
0.08
0.1
0.2
0.4
0.6
β

Usually these effects are taken into account in eikonal approximation (elastic rescatterings only)

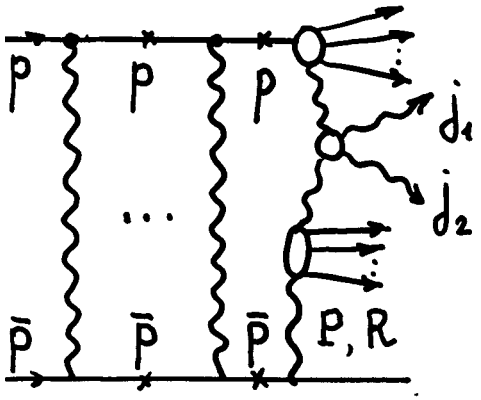

The suppression factor (survival probability)

$$S^2 = \frac{\int |M(s,b,..)|^2 e^{-\Omega(b)} d^2b}{\int |M(s,b,..)|^2 d^2b}$$

However inelastic intermediate states can play an important role.

see also GLM

Eigen states with small absorption will lead to smaller suppression

Consider this effects in the 2-channel model KMR model (for details see)

V. Khoze, A. Martin, M. Ryskin : KMR

Eigen states absorption cross sections differ strongly (3÷4 times)

In partonic model they correspond to configurations of differen sizes

Large size - large σ - state 1

Small(er) size - smaller σ - state 2

Next step: relation to partonic configurations with different x. KKMR

Small size - mostly valence quarks
$x \sim 1$

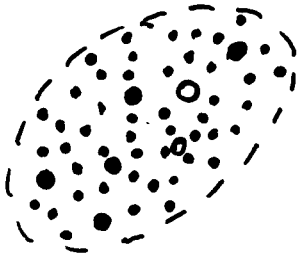

Large size - mostly gluons and sea
$x \ll 1$

In this approach it is possible to explain diffractive production of jets at Tevatron CDF

Not only an absolute magnitude but also β-dependence differs from predictions, based on HERA data (Note β^{-1} behaviour of CDF data for small β) Fig. K. Goulianos

Kinematics: $\bar{\xi} = 0.06 \quad M^2 = \bar{\xi} \cdot S = 2 \cdot 10^5 \text{ GeV}^2$

$$M_{jj}^2 = x_1 \beta M^2 \sim 10^3 \text{ GeV}^2$$

$$x_1 \cdot \beta \approx 5 \cdot 10^{-3}$$

$\beta \gtrsim 0.25 \rightarrow x_1 \lesssim 0.02$ mostly gluons

$\beta \sim 0.025 \rightarrow x_1 \sim 0.2$ mostly valence q

Thus in this model suppression factor increases as β decreases (for CDF kinemat.)

In this model it is possible to reproduce CDF results without free parameters. Fig.

KKMR (2001)

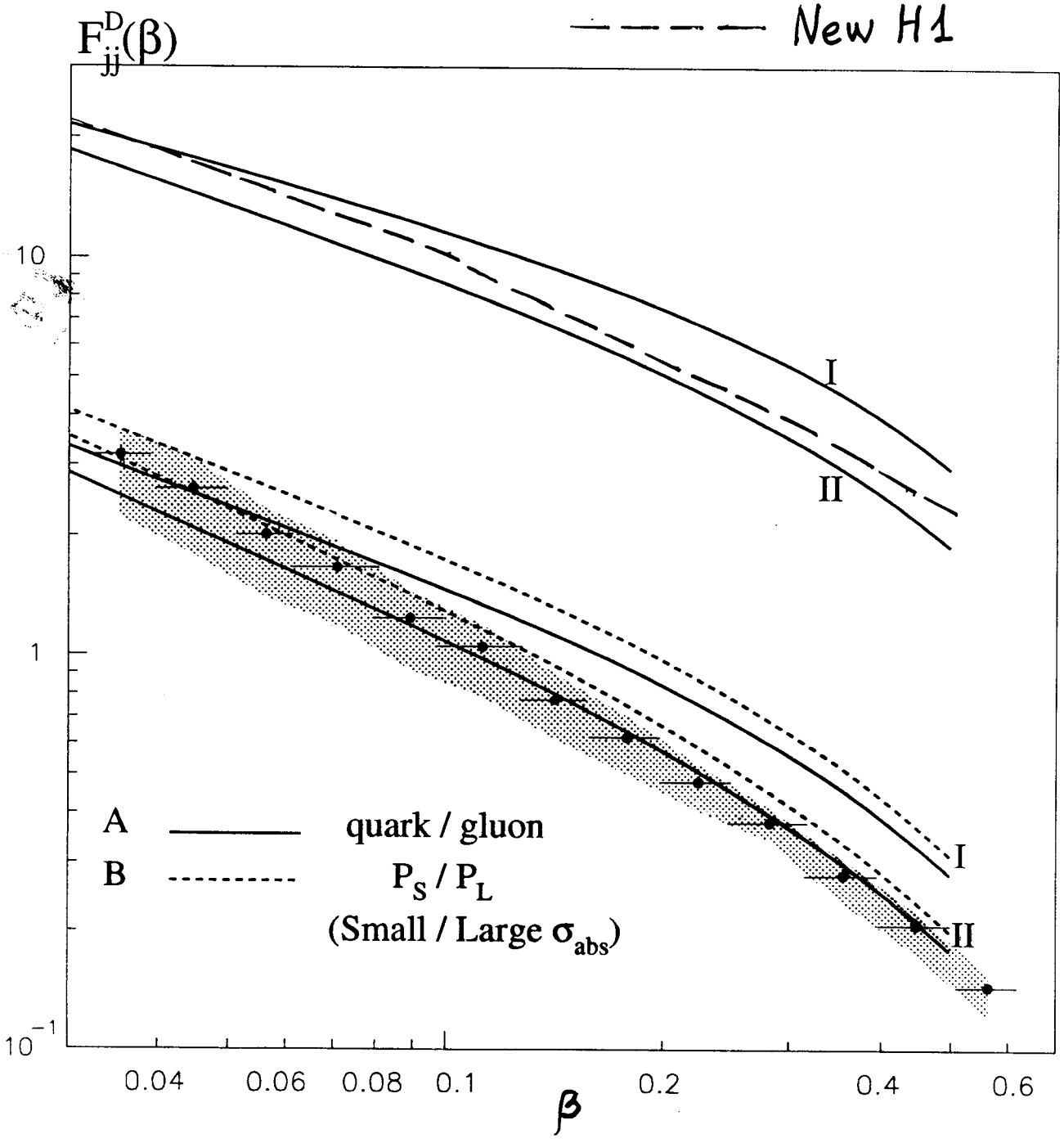
$F_{jj}^{D}(\beta)$
New H1
10
1
10^{-1}
I
II
I
II
A
quark / gluon
B
P_S / P_L
(Small / Large σ_{abs})
0.04
0.06
0.08
0.1
0.2
0.4
0.6
β

Some consequences:

a) At much higher energies (LHC) the shape of β-distribution will be closer to HERA result

b) For W-production at Tevatron suppression is smaller (≈ 0.2).

c) For processes mediated by gluons (at small x) like $b\bar{b}$, J/ψ, ... suppression is stronger ($0.06 \div 0.1$).

d) Change of suppression factor with x of a parton helps to understand results on two high p_T jets separated by a large rapidity gap

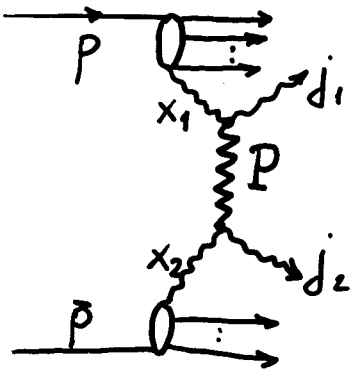

Suppression increases as x_i decrease (Suggested by D$_0$ data)

$$R_{1800}^{630} = \frac{f_s^{630}}{f_s^{1800}} = 3.4 \pm 1.2$$

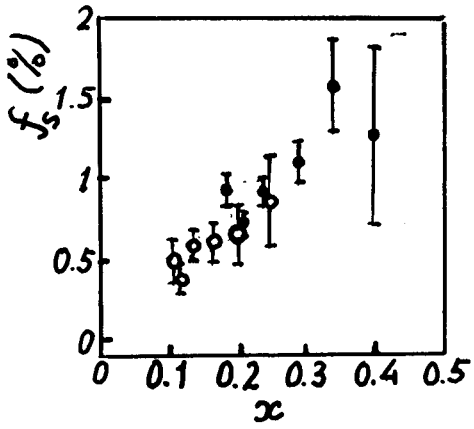

Jets in diffractive photoproduction and DIS.

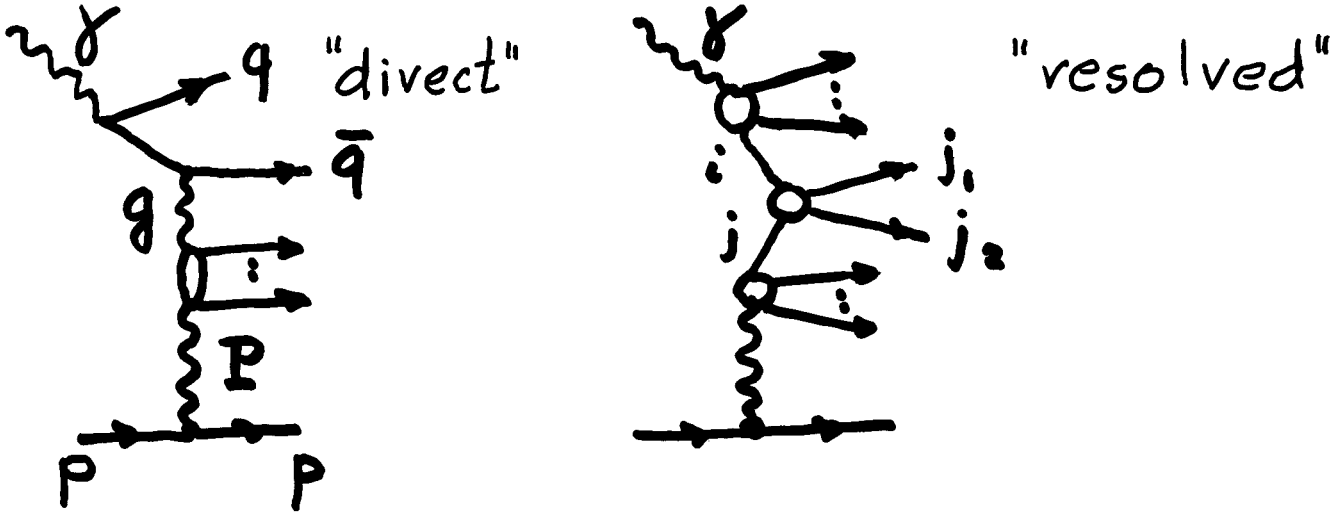

"Divect" component has a small size and little absorption. $x_\gamma \approx 1$

"Resolved" is absorbed in photoprod.

Small effect in DIS.

Problem in photoproduction

To avoid problems with higher order corrections use ratios

$$R = \frac{d\sigma_D^{jj}}{d\sigma_{inc}^{jj}} = \frac{\tilde{F}_P^g(x_g,\mu^2)}{x_g f_p^g(x_g,\mu^2)} \left| S(x_\gamma, Q^2) \right|^2$$

$$\tilde{F}_P^g(x_g,\mu^2) = F_P(x_P) \otimes f_P^g(\beta,\mu^2)$$

K K M R (2003)

(20)

KKMR (2003)

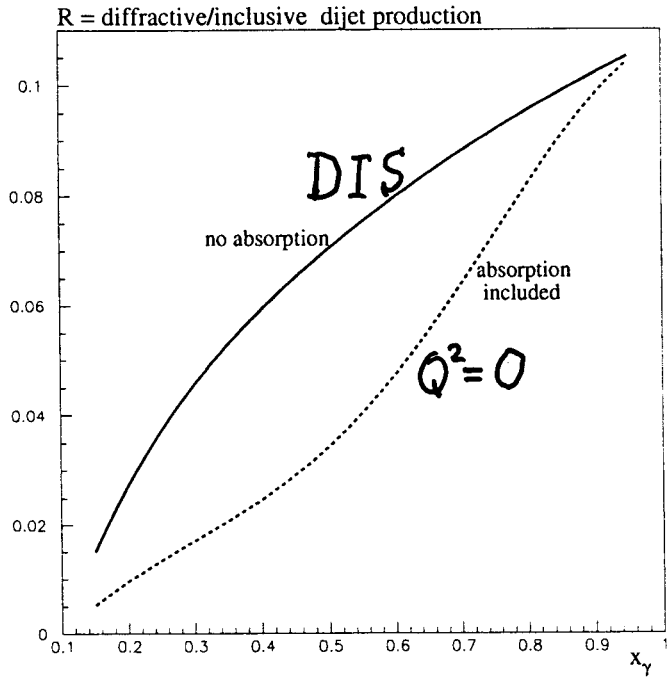

Figure 6: The predictions for the ratio, R, of diffractive and inclusive dijet photoproduction at HERA, of (4), as a function of x_γ. The curves have been calculated using the Pomeron flux and gluon distribution in the Pomeron of Refs. [13], and correspond to a γ-proton c.m. energy $W = 205$ GeV, dijet mass $M_{12} = 12$ GeV, $x_P^{\rm max} = 0.03$ and scale $\mu^2 = 15$ GeV^2. For the gluon distribution in the proton we conservatively use that of CTEQ6M partons [16]. The use of the MRST2001 or MRST2002 [17] gluons gives a value of R which is a bit larger. The predictions based on single-Pomeron and multi-Pomeron exchange are shown as continuous and dashed curves respectively. The ratio R of the high Q^2 processes is not expected to have absorptive corrections, and hence should follow the continuous curve.

This method has been used by ZEUS for study of dijet produced with forward neutrons (mostly π-echange).

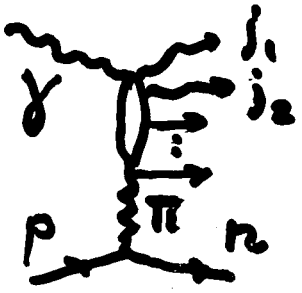

Data confirm a suppression of "resolved" component (Fig.)

Note that R in DIS indicates an amount of shadowing for gluons in the proton

$R \approx$

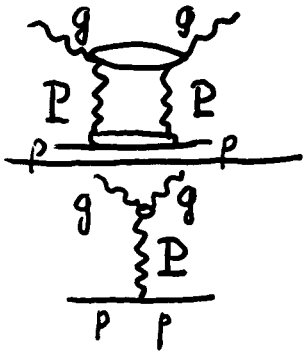

(for small R)

R increases fast as $x \to 0$ and exceeds unitarity limit already in HERA region. (Fig.)

Large unitarity corrections are needed (leading twist effect).

Related to "saturation" problem.

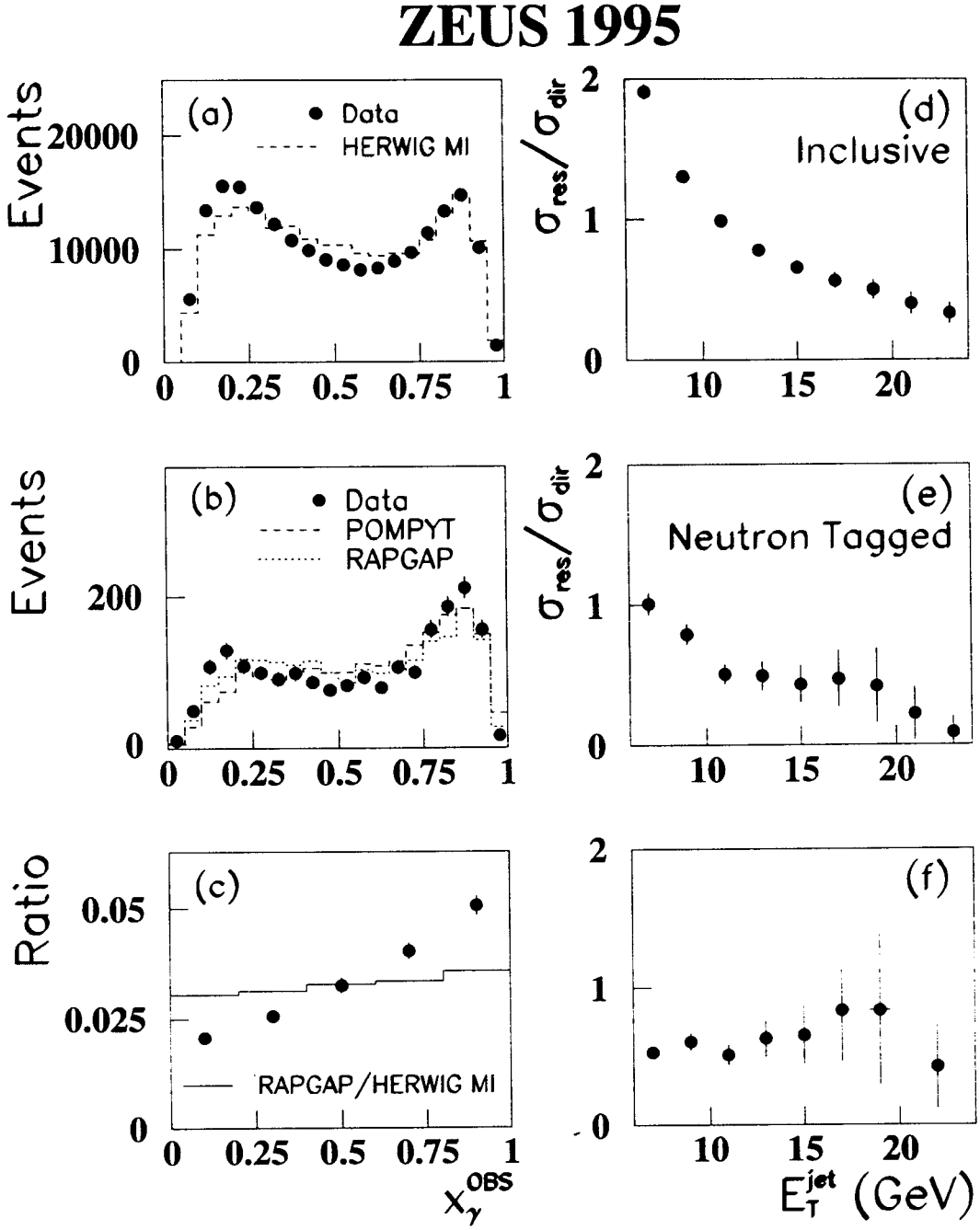

Figure 8: *The uncorrected x_γ^{OBS} distribution for (a) inclusive events compared to the expectations of HERWIG with multiple interactions, and (b) for neutron-tagged events compared to the expectations of POMPYT and RAPGAP. The ratio of the neutron-tagged to inclusive x_γ^{OBS} distributions is shown in (c) together with the ratio of RAPGAP to HERWIG MI. The Monte Carlo predictions are area normalized to the data in (a,b) and normalized at $x_\gamma^{OBS} = 0.5$ in (c). The ratio of the resolved to direct cross sections as a function of E_T^{jet} is shown in (d) and (e) for inclusive and neutron-tagged photoproduction, respectively. Resolved (direct events) are defined by $x_\gamma^{OBS} < 0.75$ ($x_\gamma^{OBS} > 0.75$). The ratio of the ratios shown in (d) and (e), i.e. [(e)/(d)], is shown in (f). Only statistical errors are shown.*

KKMR (03

(22a)

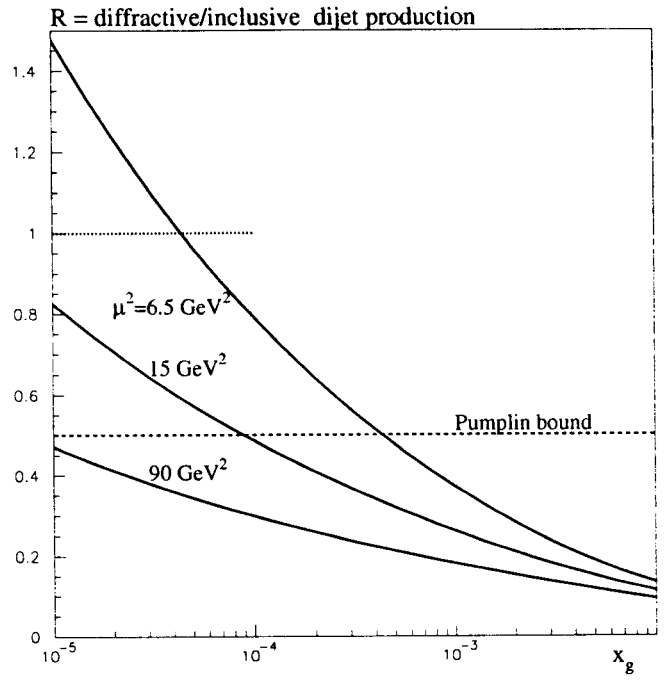

Figure 7: Predictions for the ratio R of diffractive and inclusive dijet production, of (4), shown as a function of x_g for different scales μ^2, with $x_P^{\max} = 0.1$. Absorptive corrections are neglected.

for quite a range of virtualities μ^2. This means that the application of the single Regge pole approximation in the small x region is not valid and leads to a violation of unitarity. The diagrams of Fig. 5, which take into account multi-Pomeron exchanges, must be included (as, for example, has been done in Ref. [23]) in order to ensure that $R < 1$, and to restore unitarity[5].

Comparing the diagrams of Figs. 5 and 4, we may say that the value of R of (4) represents the ratio of the cross section for gluon diffractive dissociation (the lower part of Fig. 5) to the total gluon–proton cross section. In analogy with hadronic interactions, it is reasonable to believe that diffractive processes are less than one half of the total gluon–proton cross section [25], and thus that $R \leq \frac{1}{2}$. From Fig. 7 we see that, for gluons, this bound is already exceeded for $x_g \sim 10^{-4}$. Moreover, the violation of unitarity appears in this region of x_g over a large interval of μ^2. This is related to the fact that the diffractive production of states with small β is not a high-twist effect. Note that here we discuss the absorptive effect caused by the rescattering of intermediate partons (described by the multi-Pomeron exchange contributions shown in Fig. 5), and not the rescattering of the fast constituents of the photon. The rescattering of intermediate partons takes place at scales much smaller than the hard scale μ^2. The main origin of the large

[5]See also the discussion of this problem in Ref. [24].

• Double Pomeron jet production

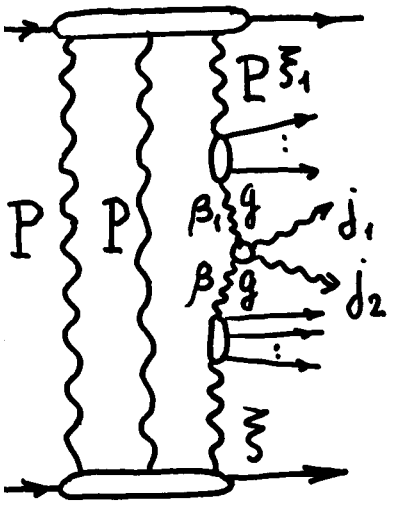

This process is observed at Tevatron

Test of factorization by CDF

$$R_1 = \frac{d\sigma^{jj}_{SD}}{d\sigma^{jj}_{in}} = \frac{F_P(\xi)\cdot f^g_P(\beta)}{x\cdot f^g_p(x)}\,|S_1|^2$$

$x = \xi\cdot\beta$

$$R_2 = \frac{d\sigma^{jj}_{DP}}{d\sigma^{jj}_{SD}} = \frac{F_P(\xi_1)\cdot f^g_P(\beta_1)}{x_1 f^g_p(x_1)}\,\frac{|S_2|^2}{|S_1|^2}$$

$x_1 = \xi_1\cdot\beta_1$

$$\frac{R_1}{R_2} = \frac{F_P(\xi)\, f^g_P(\beta)\, x_1 f^g_p(x_1)}{F_P(\xi_1)\, f^g_P(\beta_1)\, x f^g_p(x)}\cdot\frac{(|S_1|^2)^2}{|S_2|^2}$$

KKMR (PL. 2003)
A. Bialas, R. Peschanski

if $\xi=\xi_1$, $\beta=\beta_1$ $(x=x_1)$

$$R \equiv R_1/R_2 = (|S_1|^2)^2/|S_2|^2$$

For single Regge exchange $(|S_i^2|=1)$

$$R = 1$$

With account of absorption

$$|S_1|^2 = 0.1\,,\quad |S_2|^2 = 0.05$$

$$R = 0.2$$

KMR

Note that $|S_2|^2 \neq |S_1|^2$

$$R_{exp} = 0.19 \pm 0.07$$

• Estimates of the cross section for DPE Higgs production

H couples to $\gamma\gamma$, gg

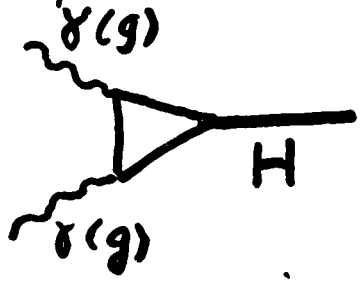

So it can be produced in $\gamma\gamma$ collisions or in pp by $\gamma\gamma$ fusion

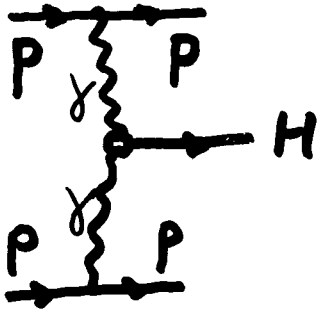

Small σ (except for very small $p_\perp^2 \lesssim 10^{-3}\ GeV^2$)

Production by gluons

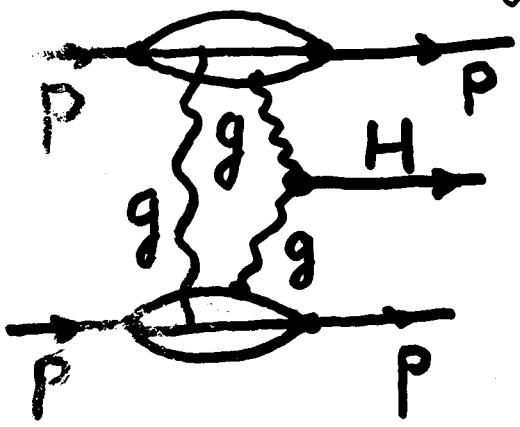

A. Schäffer, O. Nachtmann, R. Schöpf (1990)

A. Bialas, P.V. Landshoff (1991)

B. Müller, A.J. Schramm (1991)

Simple estimate: $\sigma_H^{excl} \sim \sigma_H^{incl} \left(\frac{\sigma^{el}}{\sigma^{tot}}\right)^2 \sim$

$\sim 0.1\, \sigma_H^{incl}$

Large cross sections ~ 1 pb

$p_{\perp i}=0$ $\int_\Lambda^\infty \frac{d^2k_\perp}{k_\perp^6} k_\perp^2$ Soft physics ?

$k_\perp \sim \Lambda_{QCD}$

Two important effects are missing

1. Sudakov suppression

Small $k_\perp$ are suppressed for hard probe $\mu \sim M_H$

$$T \approx \exp\left(-\frac{4\alpha_s}{3\pi} \ln^2 \frac{\mu^2}{k_\perp^2}\right)$$

Small $k_\perp^2$ region is damped

$\overline{k_\perp^2} \approx 4\ \text{GeV}^2$ for $M_H = 120\ \text{GeV}$

2. Unitarity effects:

survival probability not to have inelastic multiparticle production during collision.

KMR. (V.A. Khoze, A.D. Martin, M.G. Ryskin)

Calculation of cross section in QCD perturbation theory

KMR

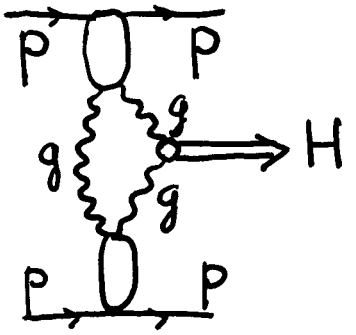

$$T_h = A\pi^2 \int \frac{d^2Q_\perp \, V_H \times}{Q_\perp^2 (\vec{Q}_\perp - \vec{P}_{1\perp})^2 (\vec{Q}_\perp + \vec{P}_{2\perp})^2}$$

$$\times f_g(x_1, x_1', Q_1^2, \mu_1^2, t) \, f_g(x_2, x_2', Q_2^2, \mu_2^2, t)$$

$$A^2 = K \frac{\sqrt{2} G_F}{9\pi^2} \alpha_s^2(m_H^2) \; ; \quad K = 1.5 \text{ NLO factor}$$

$$V_H = (\vec{Q}_\perp - \vec{P}_{1\perp})(\vec{Q}_\perp + \vec{P}_{2\perp}) \; ; \quad \mu = \frac{m_H}{2}$$

$$Q_1 = \min\{Q_\perp, |\vec{Q}_\perp - \vec{P}_\perp|\} \; ; \quad Q_2 = \min\{Q_\perp, |\vec{Q}_\perp + \vec{P}_{2\perp}|\}$$

$$x' \sim \frac{Q_\perp}{\sqrt{s}} \ll x \sim \frac{m_H}{\sqrt{s}} \ll 1 \; ; \quad x_1 x_2 = \frac{m_H^2}{s}$$

$$x_1 - x_2 = x_F^H$$

at LHC $x_i \sim 10^{-2}$

$$f_g(x, x', Q^2, \mu^2, t) = f_g(x, x', Q^2, \mu^2) \, F_N(t)$$

$$F_N(t) = \exp(bt) \; ; \quad b \approx 2 \text{ GeV}^{-2} \text{ from } J/\psi \text{ production at HERA}$$

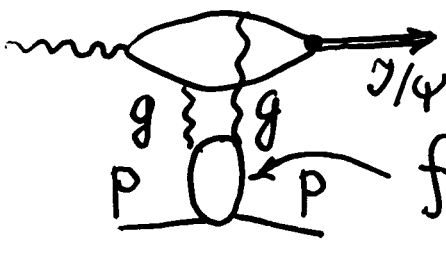

$$f_g(x, x', Q_\perp^2, \mu^2, t)$$

To single log accuracy

$$f_g(x,x',Q_\perp^2,\mu_1^2,t) = R_g \frac{\partial}{\partial \ln Q_\perp^2}\left(\sqrt{T(Q_\perp^2,\mu^2)}\, x g(x,Q_\perp^2)\right)$$

$$T = \exp\left(-\int_{Q_\perp^2}^{\mu^2} \frac{\alpha_s(k_t^2)\,dk_t^2}{2\pi\, k_t^2} \int_0^{1-\delta} dz \left[z P_{gg}(z) + \sum_k P_{qg}(z)\right]\right)$$

↑ Sudakov form-factor

$\delta = \frac{k_t}{k_t + 0.6 m_H}$; to reproduce complete one loop result

$$T \approx \exp\left(-\frac{4\alpha_s}{3\pi} \ln^2\left(\frac{\mu^2}{Q_\perp^2}\right)\right)$$

$\int \frac{d^2Q_\perp}{Q_\perp^4} T(Q_\perp^2,\mu^2)$ is not sensitive to small $Q_\perp^2$ region

for $\mu \sim 50$ GeV $\quad \bar{Q}^2 \approx (3 \div 4)\ \text{GeV}^2$

R_g takes into account that $x' \neq x$.

For small x it can be determined (uncertainty $\sim 4x^2$) $\quad R \approx 1.2$

$$R_g = \frac{2^{2\lambda_g+3}}{\sqrt{\pi}} \frac{\Gamma(\lambda_g + 5/2)}{\Gamma(\lambda_g + 4)} \; ; \quad g(x,Q^2) \sim \left(\frac{1}{x}\right)^{\lambda_g(Q^2}$$

$$\sigma^{(H)} = \int d^2b\, e^{-\chi(s,b)}\, \sigma_0^{(H)}(s,b,..)$$

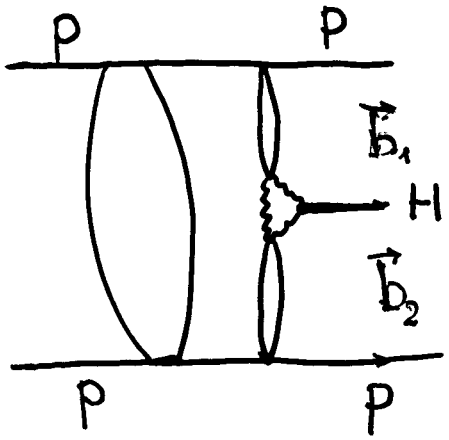

It is possible to study b-dependence by measuring $\vec{q} = \vec{p}_{3\perp} - \vec{p}_{4\perp}$ dependence $\vec{q} \leftrightarrow \vec{b} = \vec{b}_1 + \vec{b}_2$

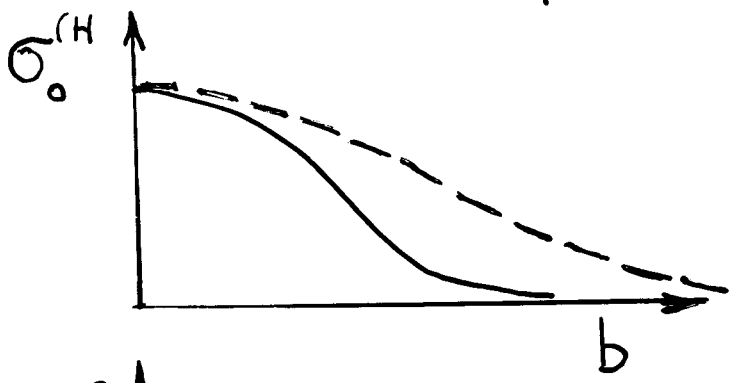

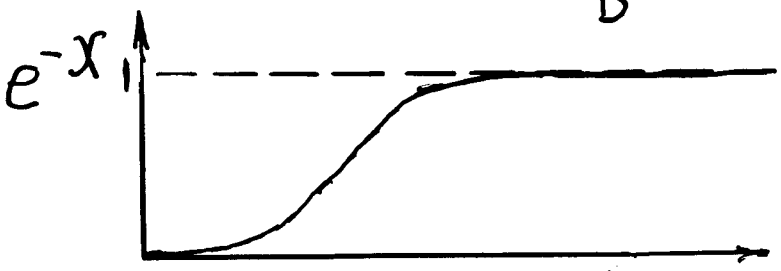

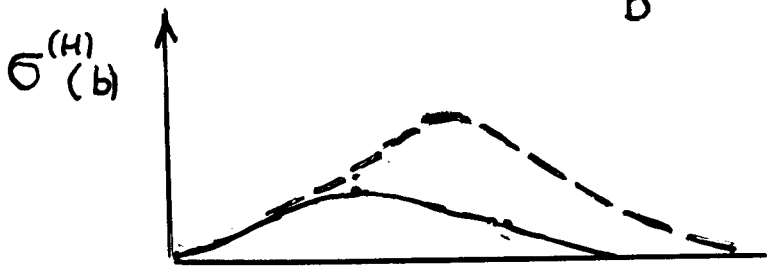

Strong reduction of cross section

"Survival probability" decreases as energy increases

at $\sqrt{s} = 1.8$ TeV $\quad |S^2| = 0.05$

$\sqrt{s} = 14$ TeV $\quad -\!\!\shortparallel\!\!- \approx 0.026$

Final results for SM Higgs ($M = 120$ GeV)

$\sigma =$ 0.2 fb Tevatron ← Proposal by M. G. Albrow, A. Rostovtsev (2000)

3 fb LHC

Small cross sections, but very clean signal due to suppression of background

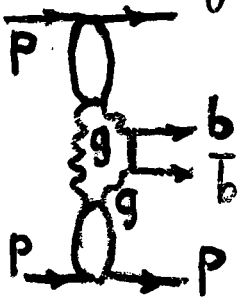

For small $t_1, t_2 < 1$ GeV^2 $b\bar{b}$-system is produced in $J_z = 0$ state. KMR

$$\text{Suppression} \sim \frac{m_b^2}{E_t^2} \sim 10^{-2}$$

$\frac{S}{B} \approx 3 \div 4$; for $\Delta M \approx 1$ GeV

Extension to MSSM

3 neutral Higgs bosons $\underbrace{h, H}_{0^+}, \underbrace{A}_{0^-}$

$m_h \lesssim 135$ GeV

$tg\beta = \frac{v_2}{v_1}$

Intense coupling regime of MSSM

$tg\beta \gg 1$, $m_h \approx m_H \approx m_A$

$\gamma\gamma$, WW^*, ZZ^* modes are suppressed

Strong ($\sim tg\beta$) coupling to $b\bar{b}$

Large $gg \to h, H, A$ couplings. —
— large cross sections

h and H in this limit can be easily observed at LHC. (Fig.)

If a state is observed in DPE it has: $Q=0$, $C=+$, $P=+$ ($P=-$ small σ), color neutral

Possibility to study different decay modes and to determine branching ratios.

Search for hard exclusive DPE process at Tevatron

$$p\bar{p} \to p\, jj\, \bar{p}\ ,\quad p\bar{p} \to p\, X_c\, \bar{p}$$

$\sigma^{jj}_{th}(E_T^j > 25\ GeV) \approx 40\ pb$

$\sigma^{jj}_{ex} \leq (34 \pm 5 \pm 10)\ pb$ recent CDF results are consistent with theor predictions

$\left.\frac{d\sigma^{th.}_{\chi_c^0}}{dy}\right|_{y=0} = 130\ nb$

Central exclusive diffractive production

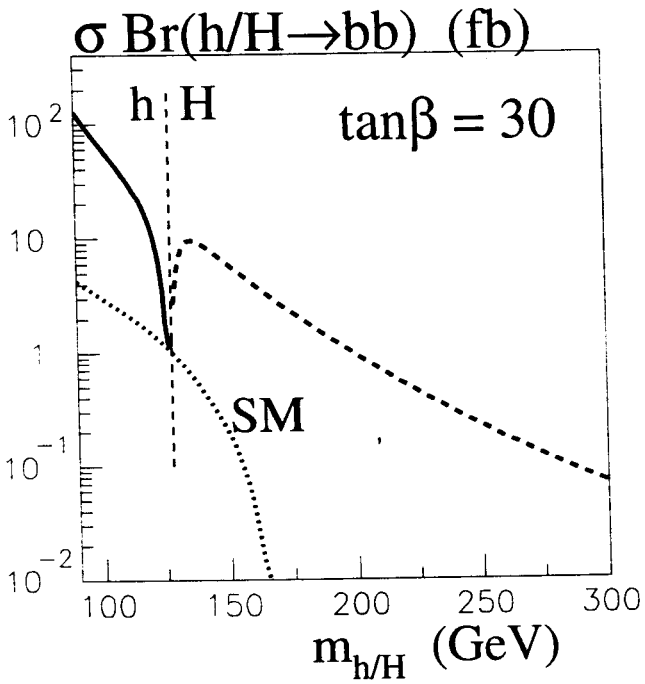

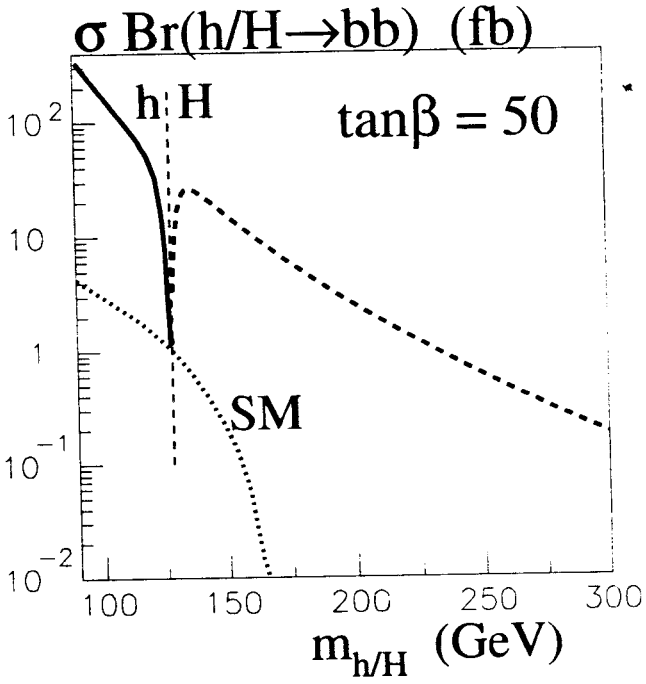

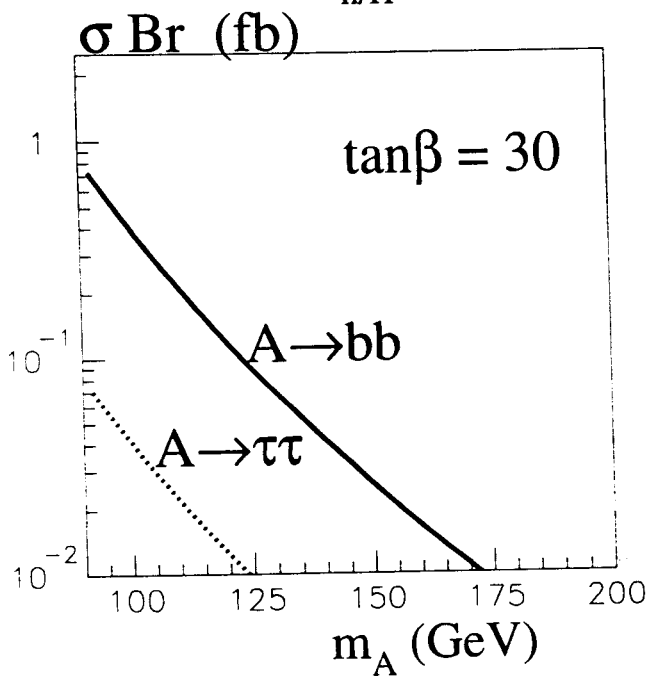

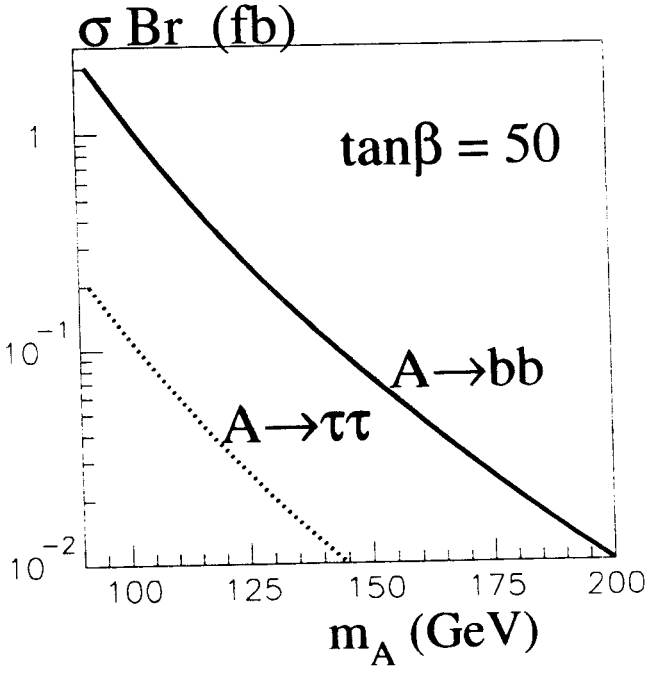

- Double pomeron exchange as spin-parity analyzer

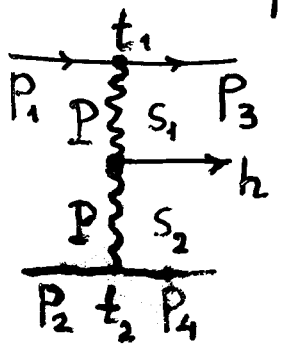

$t_1 = -p_{3\perp}^2 \; ; \; t_2 = -p_{4\perp}^2$

$$T = g_{13}(t_1)\, g_{24}(t_2) \left(\frac{S_1}{S_0}\right)^{\alpha_I(t_1)} \left(\frac{S_2}{S_0}\right)^{\alpha_I(t_2)} \times \zeta_{\alpha_I}(t_1)\, \eta_{\alpha_I}(t_2)\, g_{PP}^{h\lambda}(p_{3\perp}^2, p_{4\perp}^2, \vec{p}_3 \vec{p}_4)$$

K. Boreskov (1970)

Structure of the $g_{PP}^{h\lambda}$ vertex depends on quantum numbers of h. λ-helicity

φ - angle between $\vec{p}_{3\perp}$ and $\vec{p}_{4\perp}$

0^+ dependence on φ is determined by dynamics (weak for Higgs boson)

0^- $g_{PP}^{h} = f_{0^-}(p_{3\perp}^2, p_{4\perp}^2, \vec{p}_3 \vec{p}_4)\, \varepsilon^{ikl}\, p_{3\perp i}\, p_{4\perp k}\, n_{0l}$

$\vec{n}_0$ direction of colliding protons

$$\frac{d\sigma}{dt_1 dt_2} \sim t_1 t_2 \sin^2\varphi$$

1^+ $g_{PP}^{h} = f^0 \cdot \varepsilon^{ikl}\, p_{3\perp i}\, p_{4\perp k}\, e_l^h + f^1 (p_{3\perp} - p_{4\perp})_i\, n_{0k}\, e_e^h\, \varepsilon^{ikl}$

Due to PP-symmetry $f^0 \sim (p_{3\perp}^2 - p_{4\perp}^2)$ - small for small t_1, t_2

Observations of WA102 Collaboration

Interpretation by F. Close et al.

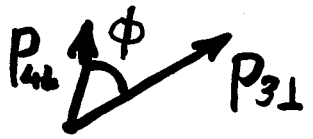

WA102

$P_1 + P_2 \rightarrow P_3 + h + P_4$

Correlations between transverse momenta of produced protons

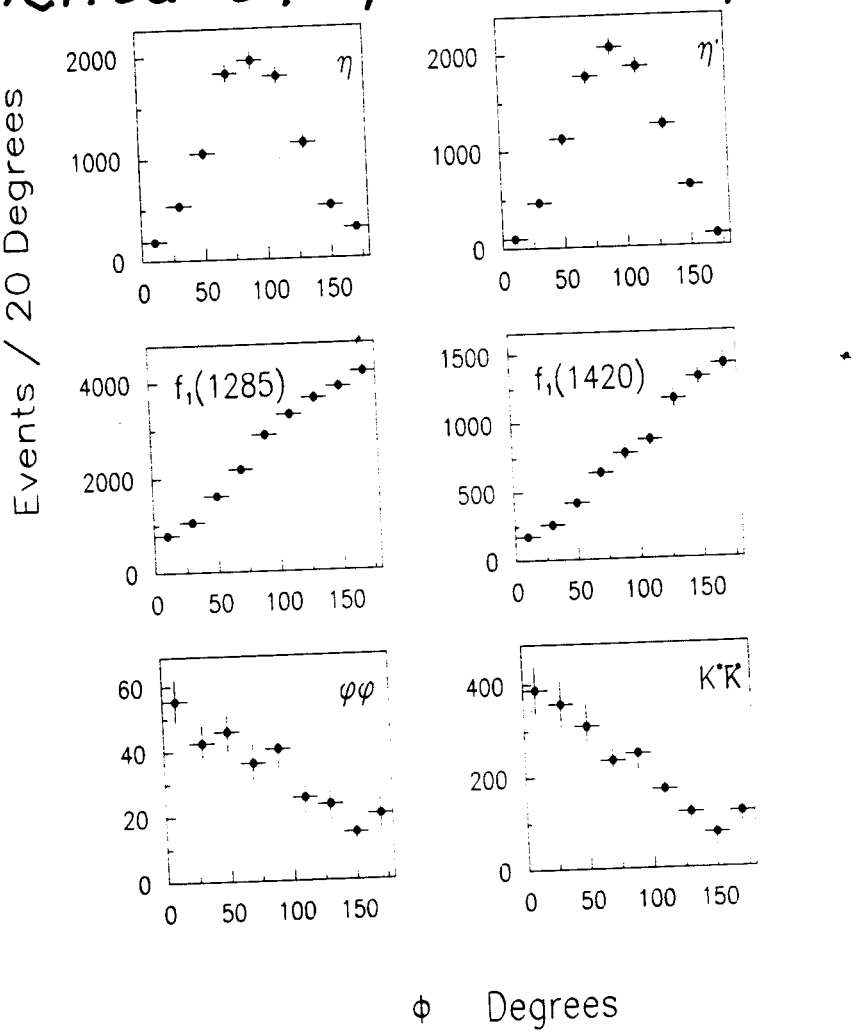

Figure 4: The azimuthal angle between the fast and slow protons (ϕ) for various final states.

it is completely determined [SGMR]. The apparent infrared divergence of (21) is nullified for $h(0^+)$ production by the Sudakov factors embodied in the gluon densities f_g. However the amplitude for $h(0^-)$ production is much more sensitive to the infrared contribution. Indeed let us consider the case of small $p_{i\perp}$ of the outgoing protons. Then, from (22), we see that $V_{h(0^+)} \sim Q_\perp^2$, whereas $V_{h(0^-)} \sim p_{3\perp} p_{4\perp}$ (since the linear contribution in $Q_\perp$ vanishes after the angular integration). Thus the $d^2Q_\perp/Q_\perp^4$ integration for $h(0^+)$ is replaced by $p_{3\perp}p_{4\perp}d^2Q_\perp/Q_\perp^6$ for $h(0^-)$, and now the Sudakov suppression is not enough to prevent a significant contribution from the $Q_\perp^2 \lesssim 1$ GeV^2 domain.

To explore the infrared sensitivity we use GRV partons [GRV98], which extend to the relatively low scale of $Q^2 = 0.8$ GeV^2. In Fig. 4 we compare the results for the ϕ dependence of

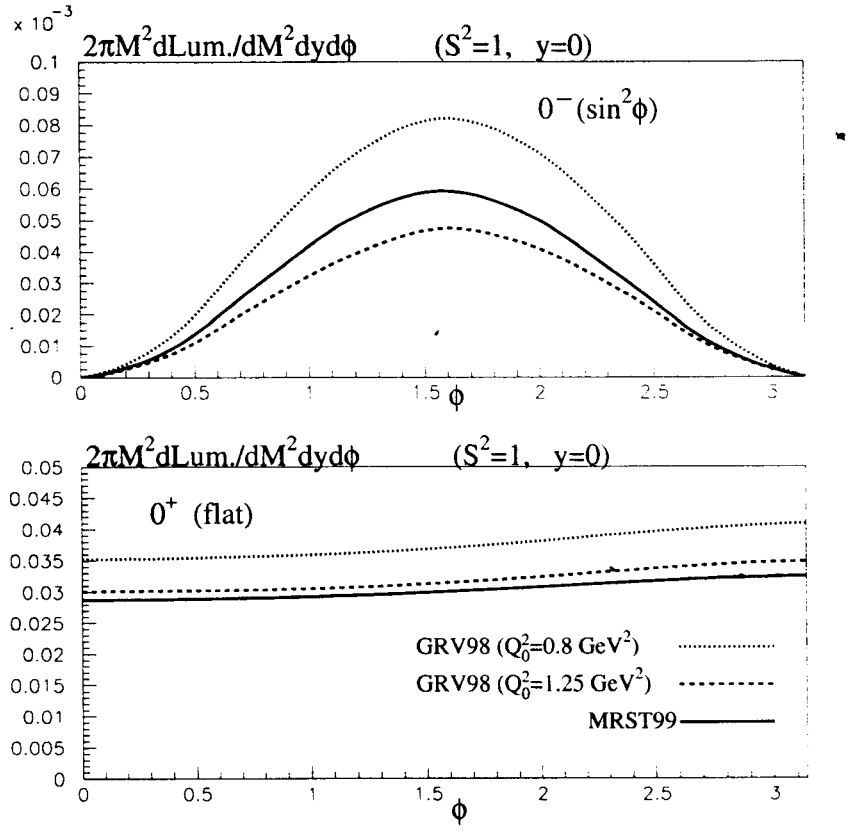

Figure 4: The ϕ dependences of diffractive exclusive $h(0^+)$ and $A(0^-) \equiv h(0^-)$ production, $pp \to p + h + p$, at the LHC, with $m_h = 120$ GeV. ϕ is the angle in the transverse plane between the outgoing protons. The curves are for central rapidity and do not include absorptive corrections. They correspond to the effective luminosities for the $gg \to h(0^\pm)$ subprocesses integrated over the outgoing proton momenta $\vec{p}_{i\perp}$, assuming an $\exp(-bp_{i\perp}^2)$ behaviour of the unintegrated gluon densities f_g, with slope $b = 2$ GeV^{-2}.

Conclusions

- Investigation of diffractive processes at LHC will provide an important information on dynamics of hadronic interactions at superhigh energies.
- Unitarity effects are important for understanding of diffraction at these energies.
- DPE production of Higgs bosons can be studied at LHC with a good signal to background ratio. Good possibilities for study of MSSM Higgs bosons in DPE.